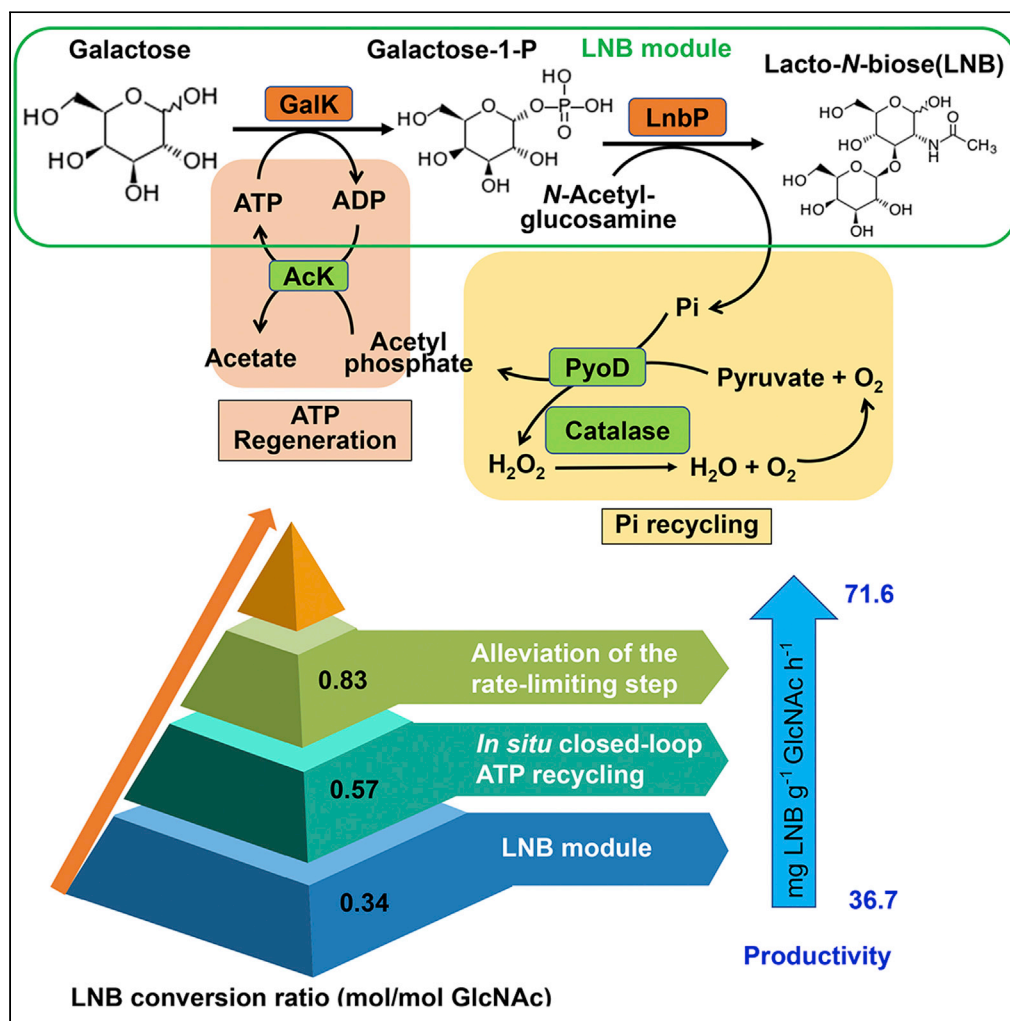


Article

Lacto-*N*-biose synthesis via a modular enzymatic cascade with ATP regeneration

Zhiqiang Du,
Zhengyao Liu,
Yinshuang Tan,
Kangle Niu, Wei
Guo, Yangyang
Jia, Xu Fang

fangxu@sdu.edu.cn

HIGHLIGHTS

Introducing an ATP recycling system improved LNB production efficiency

In situ ATP recycling fulfilled by combining pyruvate oxidase with acetate kinase

LNB yield reached 0.96 mol/mol GlcNAc, whereas ATP addition decreased to 50%

Article

Lacto-*N*-biose synthesis via a modular enzymatic cascade with ATP regenerationZhiqiang Du,¹ Zhengyao Liu,¹ Yinshuang Tan,¹ Kangle Niu,¹ Wei Guo,¹ Yangyang Jia,³ and Xu Fang^{1,2,3,4,*}

SUMMARY

Human milk oligosaccharides (HMOs), the third most abundant solid component of human milk, are reported to be beneficial to infant health. The biosynthesis of lacto-*N*-biose (LNB), the building block for HMOs, suffers from excessive addition of cofactors and intermediate inhibition. Here, we developed an *in vitro* multienzyme cascade composed of LNB module, ATP regeneration, and pyruvate oxidase-driven phosphate recycling to produce LNB. The integration between ATP regeneration and Pi alleviation increased the LNB conversion ratio and resulted in a ΔG° decrease of 540 KJ/mol. Under optimal conditions, the LNB conversion ratio was improved from 0.34 to 0.83 mol/mol GlcNAc and the ATP addition decreased to 50%. Finally, 0.96 mol/mol GlcNAc and 71.6 mg LNB g⁻¹ GlcNAc h⁻¹ of LNB yield was achieved in a 100-mL reaction system. The synergistic strategy not only paves the way for producing LNB but also facilitates other chemicals with multienzyme cascades.

INTRODUCTION

Breast milk is considered to be the gold standard for nutrition in infants (Lyons et al., 2020). Human milk oligosaccharides (HMOs), the third most abundant solid ingredient in breast milk, play pivotal roles in prebiotics for intestinal probiotics, maturation of the baby's intestinal immune system, and protection against pathogenic infections (Eriksen et al., 2018). Moreover, HMOs have been approved in the United States (GRAS, FDA), Europe (NF regulation, EFSA), Australia, etc., as food additives especially in neonate formulas (Bych et al., 2019; Li et al., 2020).

Until recently, the limited availability of HMOs has prevented their use in infant nutrition and has impeded research into their biological effects; therefore, scaled production of HMOs would be helpful in this regard. Among more than 200 HMOs (Han et al., 2012), lacto-*N*-biose (LNB), which is present in human milk, is a HMO building block and one of the bifidus growth factors (Nishimoto 2020; Thurl et al., 2010). Furthermore, LNB can be converted by lacto-*N*-biosidase into lacto-*N*-tetraose and lacto-*N*-neotetraose, which are the most abundant components and major common core structures of HMOs. It has reported that LNB and its derivatives were synthesized via chemical methods (Craft and Townsend, 2017; Hahm et al., 2016). However, the complicated steps involved in group (de)protection and stereoselectivity render it unsuitable for food products and scaled production. A food-safe and efficient biosynthetic method for the production of LNB should be developed.

Multienzyme cascade systems have the potential to achieve high catalytic efficiency, avoid the isolation of intermediates, effectively displace unfavorable reaction equilibria, and facilitate intermediate transfer and cofactors regeneration (Sperl and Sieber, 2018; Huffman et al., 2019). Nishimoto and Kitaoka (2007) reported that LNB was produced from sucrose by a multienzyme cascade system. However, the overall reaction time in the system was 600 h in the presence of an expensive cofactor, uridine diphosphate (Nishimoto and Kitaoka, 2007; Nishimoto 2020). Therefore, development of low-cost and highly efficient synthetic method for LNB biosynthesis would be worthwhile and expected.

In this study, we designed an *in vitro* synthetic enzymatic cascade pathway to produce LNB with ATP regeneration. The multienzyme cascade system contained an LNB biosynthesis module, an ATP regeneration system, and a PyoD-driven phosphate recycle module. The LNB conversion ratio was improved to 2.77-fold with an *in situ* ATP regeneration closed-loop system in the multienzyme cascade pathway. This

¹State Key Laboratory of Microbial Technology, Shandong University, Qingdao, Shandong 266237, China

²National Glycoengineering Research Center, Shandong University, Qingdao, Shandong 266237, China

³Yantai Huakangrongzan Biotechnology Co., Ltd., Yantai, Shandong 265502, China

⁴Lead contact

*Correspondence: fangxu@sdu.edu.cn

<https://doi.org/10.1016/j.isci.2021.102236>



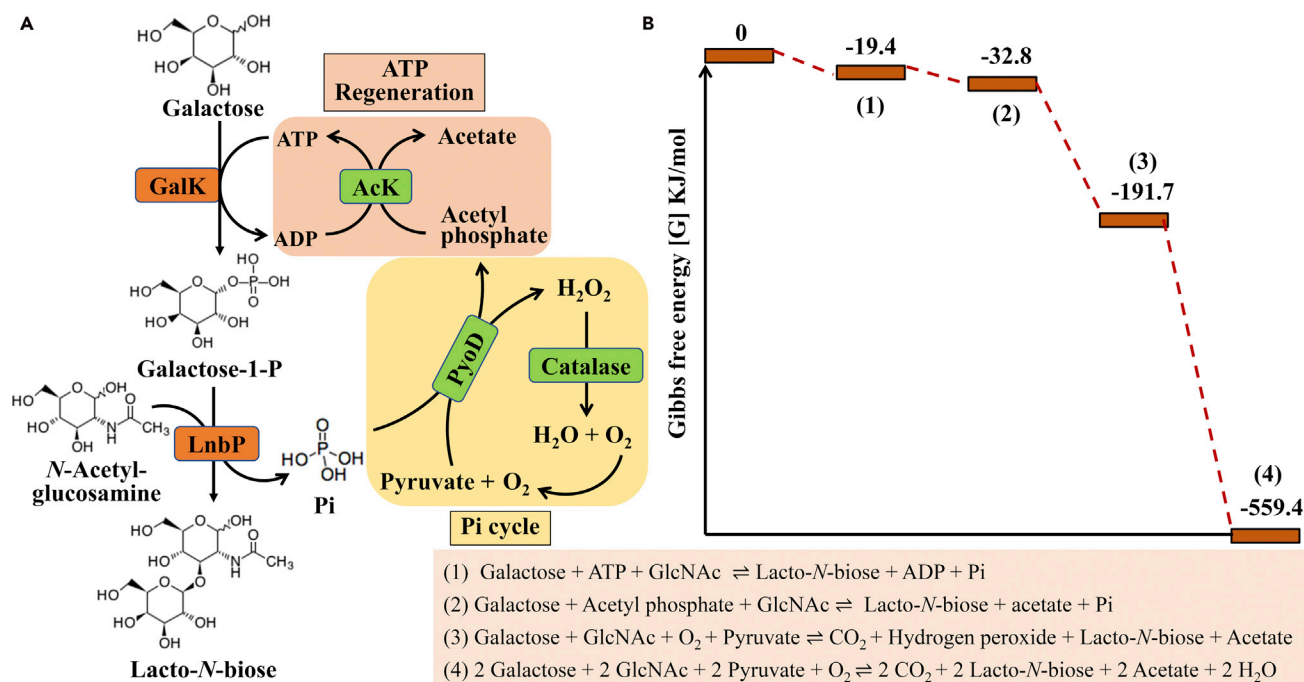


Figure 1. The design of biosynthetic pathway for the production of lacto-N-biose

(A) Scheme of an *in vitro* multienzyme system for lacto-N-biose biosynthesis from galactose.

(B) Standard Gibbs free energy change for the overall reaction. The change in the Gibbs free energy is freely available at: <http://equilibrator.weizmann.ac.il>.

Abbreviations: GalK, galactokinase; LnbP, lacto-N-biose phosphorylase; AcK, acetate kinase; PyoD, pyruvate oxidase; ATP, adenosine triphosphate; ADP, adenosine diphosphate; GlcNAc, N-acetylglucosamine; Pi, inorganic phosphate.

See also [Figures S1](#) and [S2](#).

synergistic strategy between cofactor and intermediate can be employed further in multienzyme cascade systems to facilitate the production of other chemicals.

RESULTS

In vitro multienzyme cascade pathway design

A two-step pathway has been employed for the biosynthesis of LNB from galactose (named pathway I) (Yu et al., 2010; Li et al., 2015). Typically, galactose is first converted into galactose-1-p (Gal-1p) by galactokinase (GalK, EC 2.7.1.6) in the presence of ATP, and then lacto-N-biose phosphorylase (LnbP, EC 2.4.1.211) converts Gal-1p and N-acetylglucosamine (GlcNAc) into LNB and inorganic phosphate (Farkas et al., 2000). To decrease the ΔG° in this pathway, excess expensive cofactor ATP should be added, which, however, hampered its performance. To achieve cofactor ATP cycling as is performed *in vivo*, we introduced an *in vitro* multienzyme cascade pathway for the efficient biosynthesis of LNB.

The designed multienzyme pathway (named pathway II) contains three modules (Figure 1A): (1) the LNB module: pathway I; (2) the ATP regeneration module: Acetate kinase (AcK, EC 2.7.2.1) can convert acetyl phosphate (ACP) into ATP in the presence of ADP, which can result in ATP regeneration; (3) the PyoD-driven phosphate recycle module: Pyruvate oxidase (PyoD, EC 1.2.3.3), which requires TPP and FAD as a cofactor, converts pyruvate, phosphate, and oxygen into ACP and H₂O₂. The released H₂O₂ can be converted by catalase (CAT, EC 1.11.1.6) to H₂O and oxygen, and the oxygen can be further employed in the PyoD-driven phosphate recycle module. Moreover, the synergism between modules 2 and 3 simultaneously accomplishes cofactor ATP regeneration and Pi alleviation in the designed pathway II. Particularly, the cycle between ATP, phosphate, and oxygen composes an *in situ* cofactor regeneration closed-loop system in this cascade pathway.

Furthermore, the standard Gibbs free energy change (ΔG°) for the overall reaction was determined at pH 7.0 and 0.1 M of ionic strength according to the eQuilibrator database (<http://equilibrator.weizmann.ac.il/>).

Table 1. Strains and plasmids used in this study

Strains and plasmids		
<i>E. coli</i> DH5a	Host for cloning plasmids	TransGen Biotech Co., Ltd.
<i>E. coli</i> BL21 (DE3)	Host for cloning plasmids	TransGen Biotech Co., Ltd.
pET28a	Expression vector, Km ^R	Invitrogen Co., Ltd.
pET-galk	pET28a containing <i>galk</i> gene	This study
pET-lbnp	pET28a containing <i>lbnp</i> gene	This study
pET-ack	pET28a containing <i>ack</i> gene	This study
pET-pyod	pET28a containing <i>pyod</i> gene	This study

The ΔG° decreased from -19.4 KJ/mol (reaction 1, pathway I) to -559.4 KJ/mol (reaction 4, pathway II). As shown in Figure 1B, introduction of ATP regeneration and two other recycles resulted in a decrease of 540 KJ/mol. The decreased ΔG° indicated that the overall reaction of pathway II is thermodynamically favorable for generating LNB from galactose in the *in vitro* multienzyme system.

Validation of the designed *in vitro* multienzyme cascade pathway

Based on the BRENDA and NCBI databases, we selected the enzymes GalK and AcK from *Escherichia coli* (Yang et al., 2003; Yao et al., 2019), LnbP from *Bifidobacterium bifidum* (Wada et al., 2008), and PyoD from *Aerococcus viridans* ATCC 10400 (Zhang et al., 2019) for constructing pathway II. All enzymes were expressed functionally in *E. coli* BL21 (DE3) and purified using a Ni-NTA affinity column (Table 1). As shown in Figure S1, the four enzymes were expressed and purified successfully. The specific activities of GalK, LnbP, AcK, and PyoD were 50, 1940, 70, and 45 U/mg, respectively, at 37°C (Table 2).

Proof-of-concept biosynthesis of LNB via pathways I and II was conducted (Table S1). Moreover, pathway II also contained purified AcK, PyoD and CAT to promote the regeneration of ATP. Based on the high-performance liquid chromatography and liquid chromatography-mass spectrometry results, both pathways I and II successfully produced LNB, and a 93% increase of LNB yield in pathway II-conditions I was observed compared with pathway I-conditions I (Figure S2).

Improving bioconversion efficiency of multienzyme system in pathway II

To further improve the LNB conversion, the effects of temperature, pH, Mg²⁺, and Tris-HCl concentrations on LNB production were estimated individually to obtain the optimal reaction conditions for the *in vitro* cascade system. The influence of different temperatures on LNB production was investigated at 25°C–40°C for 12 h. The highest yields of LNB were obtained at temperatures between 30°C and 37°C, and 30°C was chosen as the optimal temperature for the cascade reactions (Figure S3A). Furthermore, Figure S3A shows that there is no significant change in LNB yield between 30°C, 37°C, and 40°C. The influence of pH (6.0–8.0) on LNB production was determined at 30°C for 12 h. As shown in Figure S3B, the highest yield of LNB was obtained at pH 7.0, and higher or lower pH values were not beneficial for LNB biosynthesis. The optimal concentration of Mg²⁺ was also studied, and the highest LNB yield was obtained at 10 mM Mg²⁺ (Figure S3C). Finally, we evaluated the effect of Tris-HCl concentrations on LNB production at pH 7.0 and 30°C after a 12-h reaction, and 100 mM Tris-HCl was determined to be optimal (Figure S3D). Therefore, the optimal condition consisted of 100 mM Tris-HCl (pH 7.0); 10 mM Mg²⁺ at 30°C was chosen for the following work.

The relationship between the ATP concentration and LNB conversion ratio in the reaction was also investigated. As shown in Figure 2, the LNB conversion ratio reached 0.57 mol/mol GlcNAc in pathway II, when the added ATP concentration was increased from 2.5 to 5 mM. There was no significant improvement in LNB conversion ratio, although the ATP concentration was greater than 5 mM in pathway II. However, the LNB conversion ratio was continually improved as the ATP concentration increased in pathway I. When the ATP concentration increased from 2.5 to 10 mM in pathway I, the LNB conversion ratio was improved from 0.22 to 0.34 mol/mol GlcNAc after 12-h reaction, about 55% of that of pathway II.

Furthermore, we found that the LNB conversion ratio (0.85 mol/mol GlcNAc) under pathway II-condition IV after 96-h reaction (Figure S4) was similar to that of pathway II-condition III (Figure 4A) after 24-h reaction

Table 2. Information on the enzymes used in this study

Enzyme	EC no.	Accession no.	Source	MW (kDa)	K_m	Activity (U/mg)
Galactokinase (GalK)	2.7.1.6	AAC73844.1	<i>Escherichia coli</i> K-12 MG1655	41.5	9.6 mM [galactose]	50
Lacto- <i>N</i> -biose Phosphorylase (LnbP)	2.4.1.211	BAD80752.1	<i>Bifidobacterium bifidum</i>	84.2	39.7 mM [galactose-1-P]	1940
Acetate kinase (Ack)	2.7.2.1	AAC75356.1	<i>Escherichia coli</i> K-12 MG1655	43.3	24 mM [acetyl phosphate]	70
Pyruvate oxidase (PyoD)	1.2.3.3	A9X9K8	<i>Aerococcus viridans</i> ATCC 10400	65.5	36 mM [inorganic phosphate]	45

though the initial ATP concentration was reduced from 5 to 0.5 mM. However, the LNB conversion ratio at 0.5 mM ATP as initial concentration under pathway I-condition II only reached 0.37 after 144-h reaction and is greatly lower than that of pathway II-condition III (Figure 4A) after 24-h reaction. These results suggested that introducing the closed-loop regeneration cascade system improved the LNB yield, and that 0.5 mM ATP was sufficient for LNB biosynthesis in pathway II (Figure 2). In summary, these optimization experiments determined that the optimal reaction system consisted of 100 mM buffer (pH 7.0), 10 mM Mg^{2+} , and 5 mM ATP at 30°C (pathway II-condition I).

PyoD-driven phosphate recycling is the key step for LNB biosynthesis in the multienzyme pathway

As shown in Figure 3A, the loading amounts of enzymes including GalK, LnbP, Ack, PyoD, and CAT were individually increased 2.5- or 5-fold (2.5 or 5 U/mL). However, there was no obvious change in the LNB yield (Figure 3A). Alternatively, when the loading amounts of enzymes were individually decreased from 1.0 U/mL to 0.1 U/mL, the LNB yield greatly decreased except for CAT (Figure 3B). In particular, the LNB yield with GalK and PyoD decreased by 85% and 71%, respectively. These results suggested that the conversions from galactose to Gal-1p and from Pi and pyruvate to ACP were vital for LNB biosynthesis in the multienzyme system. The production of Gal-1p is the first step in pathway II, and the absence of Gal-1p resulted in a decrease in the reaction rate. PyoD converts pyruvate, phosphate, and oxygen into ACP and H_2O_2 .

In addition, we further investigated the relationship between the loading amount of PyoD and the Pi concentration in the reaction system (Figure 4). We found that the yield of LNB was improved significantly and the concentration of Pi was greatly decreased as the amount of PyoD increased (Figure 4). After 24 h of reaction, the Pi concentration without PyoD reached 2.99 mM and the amount of LNB produced was 0.78 g/L in control. When 20 U/mL PyoD was added in the cascade system, the concentration of Pi was reduced to less than 1 mM and the LNB production was 1.6 g/L at 24 h (Figures 4A and 4B). These results demonstrated that increased amounts of PyoD alleviated Pi inhibition for LnbP in the cascade system and improved the reaction rate.

DISCUSSION

HMOs, the third most abundant solid components in human milk, play a very important role both in infant health and in the maintenance of the adult intestinal microbiota. LNB and its derivatives, the core building blocks of HMOs, are common glycan structures in nature. Owing to the limitation of its supply, the development of an efficient and food-safe biosynthetic method is of considerable interest. Nishimoto and Kitaoka (2007) reported a one-pot enzyme cascade pathway to produce LNB from sucrose. In this pathway, 83% yield of LNB was obtained after 600 h of reaction in the presence of the cofactor UDP (Nishimoto and Kitaoka, 2007). However, each mole of synthesized LNB was accompanied by the production 1 mol fructose in this reaction, and the fructose concentration was continuously increased as the reaction time increased (Nishimoto, 2020). It is reported that high fructose concentration is unfavorable for the activity of sucrose phosphorylase (Silverstein et al., 1967). Alternatively, Yu et al. (2010) reported a two-step pathway to synthesize LNB and its derivatives with an excess supplement of ATP, and galactokinase catalyzed the conversion of galactose and ATP into Gal-1p, which was then directly converted into LNB by LnbP (Yu et al., 2010). However, a large amount of ATP was consumed to reduce the ΔG° in this pathway, so it was not suitable for scaled-up production. Because of these problems, many efforts have been employed to biosynthesize

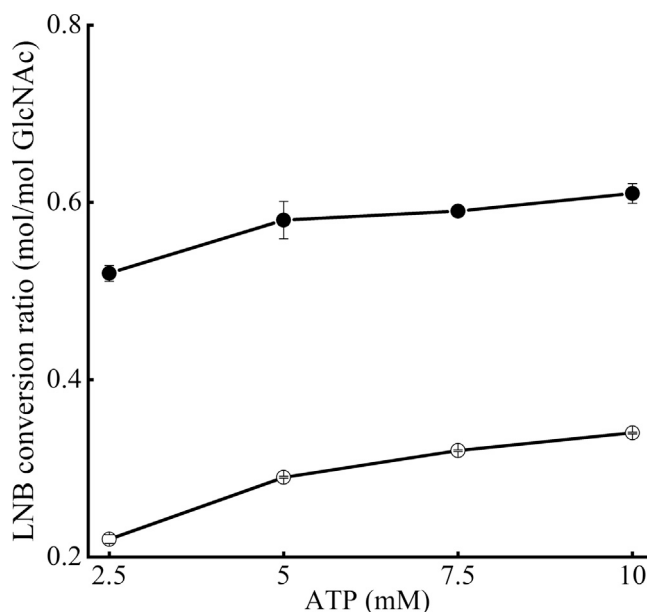


Figure 2. Influence of ATP concentration on the LNB conversion ratio in pathway I-condition I (open circle) and pathway II-condition I (closed circle) with various ATP concentration (2.5–10 mM) at 30°C for 12 h. Mean values with standard deviations (error bars) from three replicates are shown. See also [Figure S4](#) and [Table S1](#).

HMOs *in vivo* for solving the ATP supply. However, there are many challenges with regard to the production of HMOs in living cells such as low conversion efficiency, by-product production, and excess substrates for cell growth.

In this study, we aim to tackle the bottleneck by integrating ATP regeneration into the biocatalytic process to minimize the cofactor dependency and the costs in multienzyme cascade systems. Generally, three compounds including phosphoenol pyruvate (PEP), acetyl phosphate (ACP), and polyphosphate have been employed for ATP regeneration coupled with pyruvate kinase (PyK), acetate kinase (AcK), and polyphosphate kinase (PPK), respectively ([Wang et al., 2013](#)). Recently, ATP regeneration with PEP was employed in

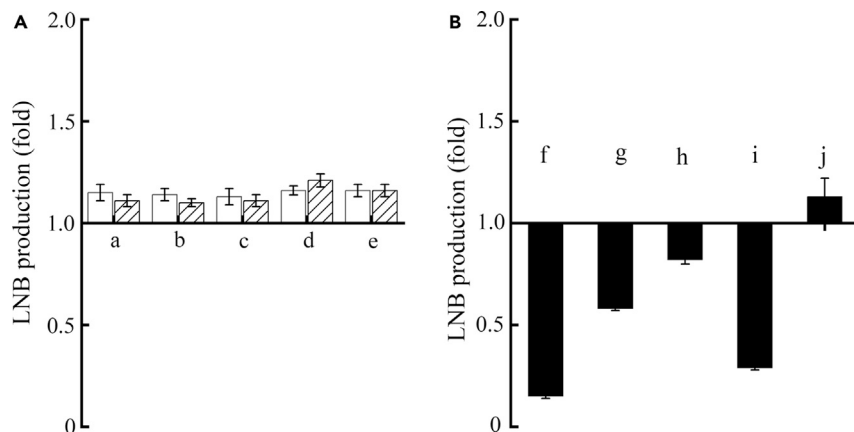


Figure 3. Influence of enzyme loading amount on LNB biosynthesis in the reaction mixture at 30°C after 12-h reaction based on pathway II-condition I. (A) Conditions a, b, c, d, and e represent GalK, LnbP, AcK, PyoD, and CAT were increased to 2.5 (blank) or 5 (hatched) U/mL, respectively; (B) Condition f, g, h, i, and j represent GalK, LnbP, AcK, PyoD, and CAT were decreased to 0.1 U/mL (dark), respectively. Mean values with standard deviations (error bars) from three replicates are shown. See also [Figure S3](#) and [Table S1](#).

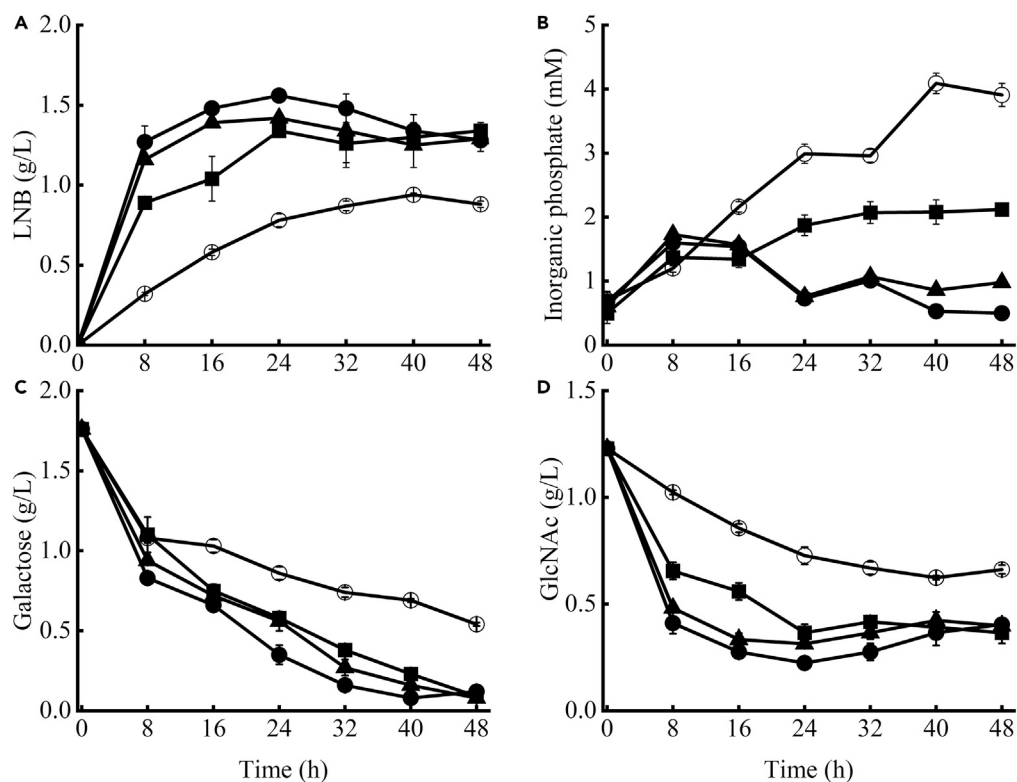


Figure 4. Time course of LNB, inorganic phosphate, galactose and GlcNAc concentrations under various loading amounts of PyoD at 30°C in pathway II-condition II. Mean values with standard deviations (error bars) from three replicates are shown.

A-D represented the concentration of LNB, inorganic phosphate, galactose and GlcNAc, respectively. The symbols (open circle, closed square, closed triangle and closed circle) represent various loading amounts of PyoD (0, 2, 10, 20 U/mL). See also Table S1.

multienzyme cascades to produce 2'-fucosyllactose (Li et al., 2020), whereas PEP is the most expensive phosphate donor for industrial applications (Andexer and Richter, 2015). It was pointed out that ACP is easily degraded in cell-free synthesis systems, which limits its further performance in multienzyme systems (Resnick and Zehnder, 2000; Ramos-Montañez et al., 2010). Owing to the availability and feasibility of PolyP, the PPK/PolyP system was considered a valuable candidate for the regeneration of ATP. However, it was demonstrated that the enzyme activity was strongly inhibited as the polyP concentration increased (Zhang et al., 2017; Strohmeier et al., 2019).

Kitaoka and Nishimoto (2017) claimed oligosaccharide biosynthesis including LNB with the design of ATP recycling system. In this study, we introduced a closed-loop cascade system to maintain the balance among ACP, ATP, and Pi concentrations through three modules in the cascade pathway. Compared with the uncycled pathway I-conditions I, the ΔG° decreased by 540 KJ/mol in pathway II (Figure 1B). As shown in Figure 5, the LNB conversion ratio improved to 0.57 mol/mol GlcNAc by introducing a modular closed-loop system compared with to pathway I-conditions I. Next, after investigating the optimal conditions for temperature, pH, and concentrations of Mg^{2+} and Tris-HCl, a 2.33-fold enhancement of the LNB conversion ratio was obtained. Finally, by elevating the enzyme ratios and loading amounts, the LNB conversion ratio reached 0.83 mol/mol GlcNAc in pathway II. Although this LNB conversion ratio is similar to the yield reported by Nishimoto and Kitaoka (2007), the reaction time was reduced to 1/55 in the present work (Nishimoto and Kitaoka, 2007). An experiment was also conducted in 100 mL reaction mixture under the optimized condition, and the LNB production was 19 g/L after 12 h of reaction (Figure S5). Finally, the LNB conversion ratio reached 0.96 mol/mol GlcNAc. The specific LNB yield was $71.6 \text{ mg LNB g}^{-1} \text{ GlcNAc h}^{-1}$, approximately 27.6-fold increase compared with that of the previous work ($2.5 \text{ mg LNB g}^{-1} \text{ GlcNAc h}^{-1}$) (Nishimoto and Kitaoka, 2007). This closed-loop regeneration system between intermediates and co-factors not only provides a promising method for scaled-up production of LNB but also sheds light on a

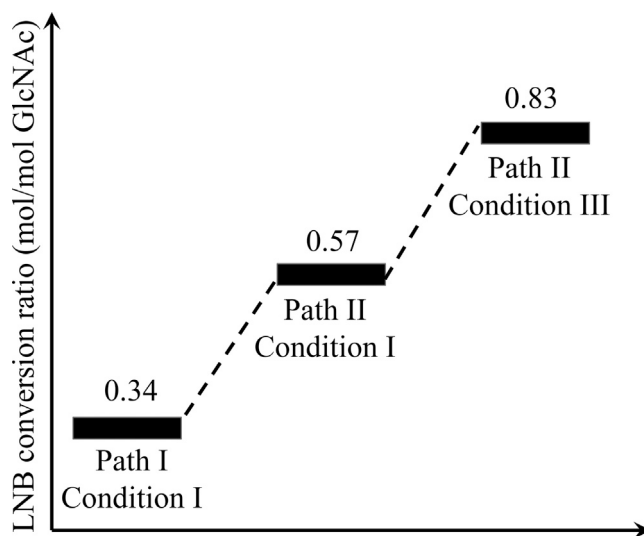


Figure 5. Increased LNB conversion ratio via manipulation of the multienzyme cascade step by step

See also [Figure S2](#), [S3](#), and [S5](#) and [Table S1](#).

strategy for ATP regeneration and offers an approach for the production of other chemicals in multienzyme cascade systems.

In summary, we designed an *in vitro* multi-enzyme cascade to biosynthesize LNB with an *in situ* ATP regeneration closed-loop system. By optimizing the reaction conditions and manipulating the rate-limiting step, the LNB conversion ratio reached from 0.34 to 0.83 mol/mol GlcNAc, when the concentration of ATP decreased to 5 mM in pathway II. The specific LNB yield was significantly improved compared with the previous work (71.6 mg LNB g⁻¹ GlcNAc h⁻¹ vs 2.5 mg LNB g⁻¹ GlcNAc h⁻¹), and 0.96 mol/mol GlcNAc was achieved in 100-mL reaction system. Thus, beyond constructing a synergistic system between ATP regeneration and intermediate recycling for LNB biosynthesis and providing an *in situ* closed-loop cofactor recycling system for multienzyme cascade, this study delivers a promising process design strategy for producing HMOs in the cell-free system.

Limitations of the study

Our study designed an *in vitro* multienzyme cascade pathway to produce LNB with an *in situ* ATP regeneration closed-loop system. We further showed that combining ATP regeneration and Pi alleviation increases the LNB conversion ratio and decreases the ATP initial concentration compared with the original pathway. However, more PyoD enzyme was employed to activate the ATP regeneration closed-loop system. For the scaled production, the high loading amount of PyoD may result in some additional cost. Further work will be carried out to improve the activity of PyoD by directed evolution ([Markel et al., 2020](#)), protein engineering ([Schmölzer et al., 2019](#); [Niu et al., 2020](#)), or screening novel enzymes ([Petroll et al., 2019](#)).

Resource availability

Lead contact

Further information and requests for resources should be directed to and will be fulfilled by the lead contact, Xu Fang (fangxu@sdu.edu.cn).

Materials availability

All reagents used in this study will be made available on request to the lead contact.

Data and code availability

The original/source data are available from the lead contact on request.

METHODS

All methods can be found in the accompanying [Transparent methods supplemental file](#).

SUPPLEMENTAL INFORMATION

Supplemental information can be found online at <https://doi.org/10.1016/j.isci.2021.102236>.

ACKNOWLEDGMENTS

The authors would like to thank Prof. Luying Xun for his valuable suggestions. We also thank Dr. Zhifeng Li and Dr. Jingyao Qu from State Key Laboratory of Microbial Technology of Shandong University for help and guidance in liquid chromatography-mass spectrometry. This study was supported by the National Key R&D Program of China (No. 2018YFA090010), China Postdoctoral Science Foundation Funded Project (2018M642645), the Qingdao Postdoctoral Application Research Project (No.2018124), the Major Program of Shandong Province Natural Science Foundation (ZR2018ZB0209), and the State Key Laboratory of Microbial Technology Open Projects Fund.

AUTHOR CONTRIBUTIONS

Z.D., Z.L., and Y.T. carried out strain construction and protein purification. Z.D., K.N., W.G., and Y.J. carried out enzyme assays. Z.D., Z.L., Y.J., and X.F. carried out optimization of multienzyme cascade reactions. Z.D. and X.F. conceived of the study and oversaw experimental work. Z.D. and X.F. designed experiments and wrote the manuscript. X.F. coordinated the project.

DECLARATION OF INTERESTS

All authors declare no conflict of interest. Part of data in this manuscript was authorized by China patent ZL201911055516.5.

Received: October 8, 2020

Revised: December 18, 2020

Accepted: February 20, 2021

Published: March 19, 2021

REFERENCES

- Andexer, J.N., and Richter, M. (2015). Emerging enzymes for ATP regeneration in biocatalytic processes. *ChemBioChem* 16, 380–386.
- Bych, K., Mikš, M.H., Johanson, T., Hederes, M.J., Vignæs, L.K., and Becker, P. (2019). Production of HMOs using microbial hosts-from cell engineering to large scale production. *Curr. Opin. Biotechnol.* 56, 130–137.
- Craft, K.M., and Townsend, S.D. (2017). Synthesis of lacto-*N*-tetraose. *Carbohydr. Res.* 440-441, 43–50.
- Eriksen, K.G., Christensen, S.H., Lind, M.V., and Michaelsen, K.F. (2018). Human milk composition and infant growth. *Curr. Opin. Clin. Nutr.* 21, 200–206.
- Farkas, E., Thiem, J., Krzewinski, F., and Bouquelet, S. (2000). Enzymatic synthesis of Gal- β -1-3-GlcNAc derivatives utilising a phosphorylase from *Bifidobacterium bifidum* 20082. *Synlett* 5, 728–730.
- Hahn, H.S., Liang, C.F., Lai, C.H., Fair, R.J., Schuhmacher, F., and Seeberger, P.H. (2016). Automated glycan assembly of complex oligosaccharides related to blood group determinants. *J. Org. Chem.* 81, 5866–5877.
- Han, N.S., Kim, T.J., Park, Y.C., Kim, J., and Seo, J.H. (2012). Biotechnological production of human milk oligosaccharides. *Biotechnol. Adv.* 30, 1268–1278.
- Huffman, M.A., Fryszkowska, A., Alvizo, O., Borra-Garske, M., Campos, K.R., Canada, K.A., Devine, P.N., Duan, D., Forstater, J.H., Grosser, S.T., et al. (2019). Design of an *in vitro* biocatalytic cascade for the manufacture of islatravir. *Science* 366, 1255–1259.
- Kitaoka, M., and Nishimoto, K. (2017). Processes for producing oligosaccharides (JP6678483B), <https://www.j-platpat.inpit.go.jp/c1800/PU/JP-2017-163881/2832CA3469A0EE7701813C3F000926B895C9F86D49769BB82EA0E5870DAC99CA/11/ja>.
- Li, C., Wu, M., Gao, X., Zhu, Z., Li, Y., Lu, F., and Qin, H.M. (2020). Efficient biosynthesis of 2'-fucosyllactose using an *in vitro* multienzyme cascade. *J. Agric. Food Chem.* 68, 10763–10771.
- Li, L., Liu, Y.H., Li, T.H., Wang, W.J., Yu, Z.K., Ma, C., Qu, J.Y., Zhao, W., Chen, X., and Wang, P.G. (2015). Efficient chemoenzymatic synthesis of novel galacto-*N*-biose derivatives and their sialylated forms. *Chem. Commun.* 51, 10310–10313.
- Lyons, K.E., Ryan, C.A., Dempsey, E.M., Ross, R.P., and Stanton, C. (2020). Breast milk, a source of beneficial microbes and associated benefits for infant health. *Nutrients* 12, 1039–1069.
- Markel, U., Essani, K.D., Besirlioglu, V., Schiffels, J., Streit, W.R., and Schwaneberg, U. (2020). Advances in ultrahigh-throughput screening for directed enzyme evolution. *Chem. Soc. Rev.* 49, 233–262.
- Nishimoto, M. (2020). Large scale production of lacto-*N*-biose I, a building block of type I human milk oligosaccharides, using sugar phosphorylases. *Biosci. Biotechnol. Biochem.* 84, 17–24.
- Nishimoto, M., and Kitaoka, M. (2007). Practical preparation of lacto-*N*-biose I, a candidate for the Bifidus factor in human milk. *Biosci. Biotechnol. Biochem.* 71, 2101–2104.
- Niu, K., Liu, Z., Feng, Y., Gao, T., Wang, Z., Zhang, P., Du, Z., Gao, D., and Fang, X. (2020). A novel strategy for efficient disaccharides synthesis from glucose by β -glucosidase. *Bioresour. Bioprocess.* 7, 45–54.
- Petroll, K., Kopp, D., Care, A., Bergquist, P.L., and Sunna, A. (2019). Tools and strategies for constructing cell-free enzyme pathways. *Biotechnol. Adv.* 37, 91–108.

Ramos-Montañez, S., Kazmierczak, K.M., Hentchel, K.L., and Winkler, M.E. (2010). Instability of *ackA* (acetate kinase) mutations and their effects on acetyl phosphate and ATP amounts in *Streptococcus pneumoniae* D39. *J. Bacteriol.* *192*, 6390–6400.

Resnick, S.M., and Zehnder, A.J.B. (2000). *In vitro* ATP regeneration from polyphosphate and AMP by polyphosphate:AMP phosphotransferase and adenylate kinase from *Acinetobacter johnsonii* 210A. *Appl. Environ. Microb.* *66*, 2045–2051.

Schmölzer, K., Weingarten, M., Baldenius, K., and Nidetzky, B. (2019). Glycosynthase principle transformed into biocatalytic process technology: lacto-*N*-triose II production with engineered exo-hexosaminidase. *ACS Catal.* *9*, 5503–5514.

Silverstein, R., Voet, J., Reed, D., and Abeles, R.H. (1967). Purification and mechanism of action of sucrose phosphorylase. *J. Biol. Chem.* *242*, 1338–1346.

Sperl, J.M., and Sieber, V. (2018). Multienzyme cascade reactions—status and recent advances. *ACS Catal.* *8*, 2385–2396.

Strohmeier, G.A., Eiteljörg, I.C., Schwarz, A., and Winkler, M. (2019). Enzymatic one-step reduction of carboxylates to aldehydes with cell-free regeneration of ATP and NADPH. *Chem Eur. J.* *25*, 6119–6123.

Thurl, S., Munzert, M., Henker, J., Boehm, G., Müller-Werner, B., Jelinek, J., and Stahl, B. (2010). Variation of human milk oligosaccharides in relation to milk groups and lactational periods. *Br. J. Nutr.* *104*, 1261–1271.

Wada, J., Ando, T., Kiyohara, M., Ashida, H., Kitaoka, M., Yamaguchi, M., Kumagai, H., Katayama, T., and Yamamoto, K. (2008). *Bifidobacterium bifidum* lacto-*N*-biosidase, a critical enzyme for the degradation of human milk oligosaccharides with a type 1 structure. *Appl. Environ. Microb.* *74*, 3996–4004.

Wang, Y.P., San, K.Y., and Bennett, G.N. (2013). Cofactor engineering for advancing chemical biotechnology. *Curr. Opin. Biotechnol.* *24*, 994–999.

Yang, J., Fu, X., Jia, Q., Shen, J., Biggins, J.B., Jiang, J.Q., Zhao, J.J., Schmidt, J.J., Wang, P.G., and Thorson, J.S. (2003). Studies on the substrate

specificity of *Escherichia coli* galactokinase. *Org. Lett.* *5*, 2223–2226.

Yao, Y.F., Ding, Q.B., and Ou, L. (2019). Biosynthesis of (deoxy)guanosine-5'-triphosphate by GMP kinase and acetate kinase fixed on the surface of *E. coli*. *Enzyme Microb. Technol.* *122*, 82–89.

Yu, H., Thon, V., Lau, K., Cai, L., Chen, Y., Mu, S.M., Li, Y.H., Wang, P.G., and Chen, X. (2010). Highly efficient chemoenzymatic synthesis of β -1-3-linked galactosides. *Chem. Commun.* *46*, 7507–7509.

Zhang, J.G., Lu, J.W., and Su, E.Z. (2019). Soluble recombinant pyruvate oxidase production in *Escherichia coli* can be enhanced and inclusion bodies minimized by avoiding pH stress. *J. Chem. Technol. Biot.* *94*, 2661–2670.

Zhang, X., Wu, H., Huang, B., Li, Z.M., and Ye, Q. (2017). One-pot synthesis of glutathione by a two-enzyme cascade using a thermophilic ATP regeneration system. *J. Biotechnol.* *241*, 163–169.

iScience, Volume 24

Supplemental information

Lacto-*N*-biose synthesis via a modular enzymatic cascade with ATP regeneration

Zhiqiang Du, Zhengyao Liu, Yinshuang Tan, Kangle Niu, Wei Guo, Yangyang Jia, and Xu Fang

Supporting Information

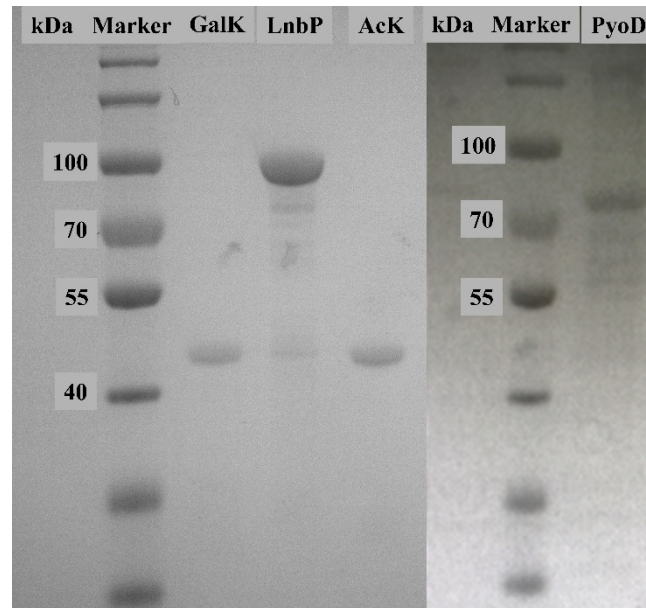


Figure S1. SDS-PAGE gel analysis of purified recombinant enzymes in cascade system. Related to Figure 1, Table 2 and Transparent Methods.

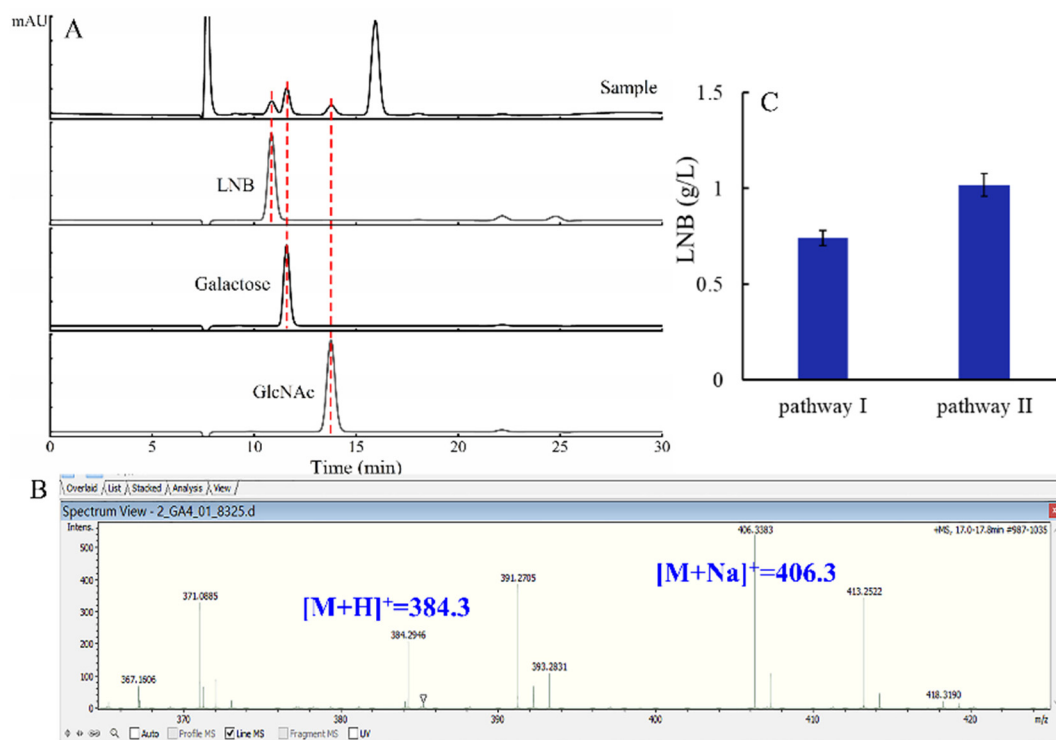


Figure S2. (A) HPLC chromatograms of lacto-*N*-biose (LNB), galactose, GlcNAc in samples. (B) HPLC-MS detection of LNB in samples. (C) The comparison in LNB biosynthesis between pathway I and pathway II. The reaction was performed in pathway I-condition I and pathway II-condition I (1 mL) at 30°C for 12 h. Mean values with standard deviations (error bars) from three repeats are shown. Related to Figure 1, Figure 5 and Transparent Methods.

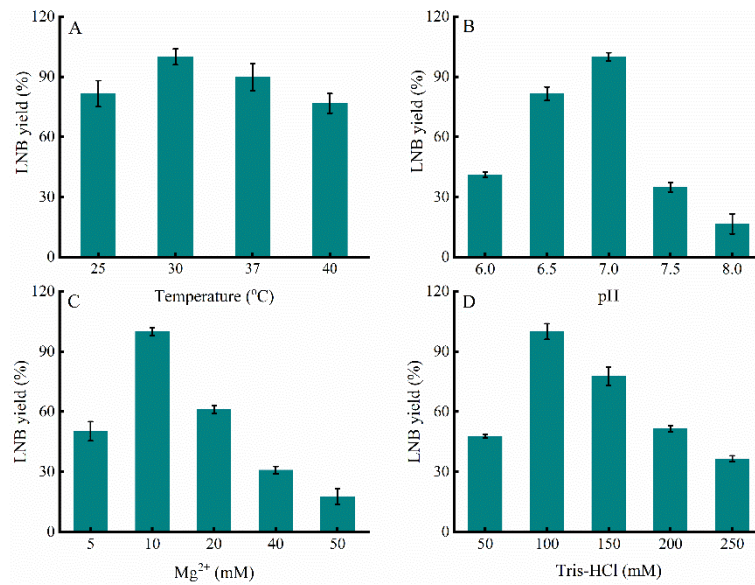


Figure S3. Optimization of reaction conditions for LNB production after 12 h of reaction. The reaction was performed in pathway II-condition I with various Tris-HCl concentration (50-250 mM), various pH 6.0-8.0, various $MgCl_2$ concentration (5-50 mM) for 12 h at various temperature (25-40°C). (A) Effects of temperature from 25-40°C on LNB production with the condition of 10 mM Mg^{2+} , pH 7.0, and 50 mM Tris-HCl. (B) Effects of pH from 6.0-8.0 on LNB production with the condition of 10 mM Mg^{2+} , 30°C, and 50 mM Tris-HCl. (C) Effects of Mg^{2+} from 5-50 mM on LNB production with the condition of pH 7.0, 30°C, and 50 mM Tris-HCl. (D) Effects of Tris-HCl concentration from 50-250 mM on LNB production with the condition of 10 mM Mg^{2+} , pH 7.0 and 30°C. Mean values with standard deviations (error bars) from three repeats are shown. Mean values with standard deviations (error bars) from three repeats are shown. Related to Figure 3, Figure 5 and Transparent Methods.

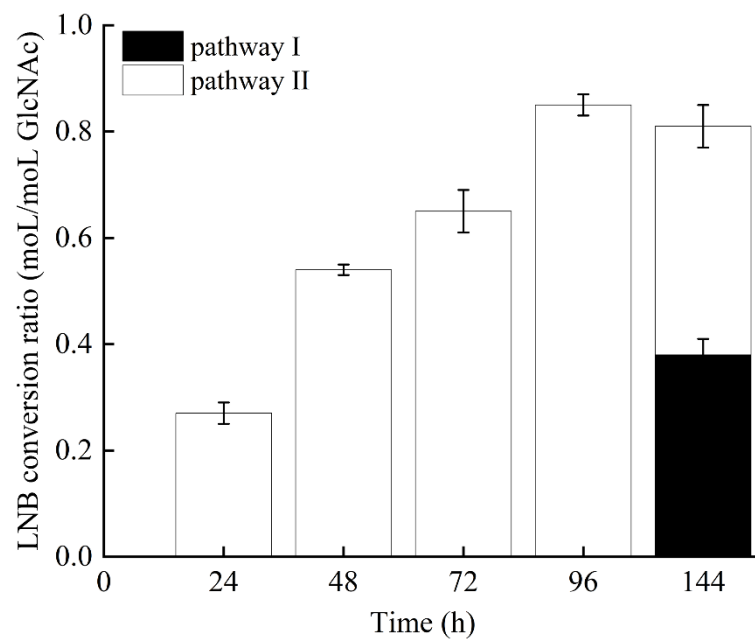


Figure S4. Time course of LNB production. The reaction was performed under pathway I-conditions II (dark) or pathway II -conditions IV (white) at 30°C. Mean values with standard deviations (error bars) from three repeats are shown. Related to Figure 2 and Transparent Methods.

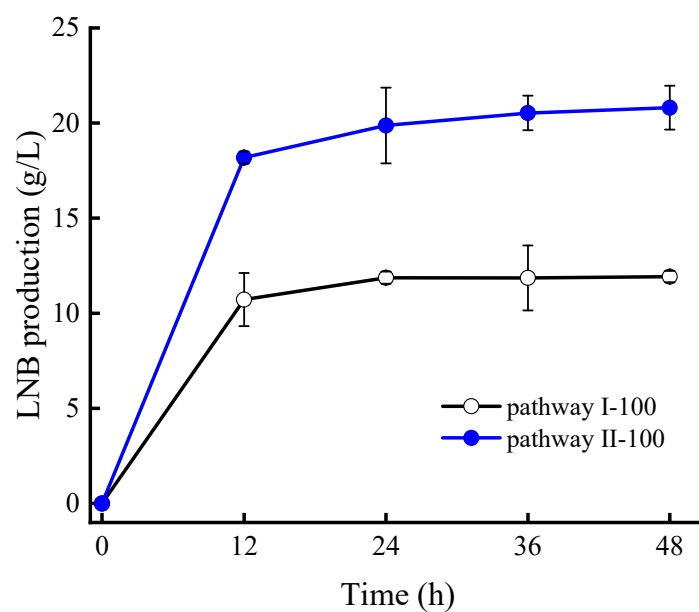


Figure S5. Time course of LNB production in 100-mL reaction mixture. The reaction was performed under the pathway I-condition (100 mM Gal, 50 mM ATP, 50 mM GlcNAc) and pathway II-conditions III at 30°C for 48 h. Mean values with standard deviations (error bars) from at least three repeats are shown. Related to Figure 5 and Transparent Methods.

Table S1. Information on the reaction conditions. Related to Figures 2-5.

	Pathway I		Pathway II			
	Condition I	Condition II	Condition I	Condition II	Condition III	Condition IV
GalK (U/mL)	1	2	1	2	2	2
LnbP (U/mL)	1	2	1	2	2	2
AcK (U/mL)	—	—	1	2	2	2
PyoD (U/mL)	—	—	1	2	10	2
CAT (U/mL)	—	—	1	2	2	2
Galactose (mM)	10	10	10	10	10	10
ATP (mM)	5	0.5	5	5	5	0.5
GlcNAc (mM)	5	5	5	5	5	5
Mg ²⁺ (mM)	10	10	10	10	10	10
Pyruvate (mM)	—	—	10	10	10	10
FAD (mM)	—	—	10	10	10	10
ThDP (mM)	—	—	30	30	30	30

Transparent methods

Materials

All chemicals were analytical grade and were obtained from Sangon Biotech, Sinopharm Chemical Reagent Co., Ltd. (Shanghai, China), or Yuanye Bio-Technology (Shanghai, China). Lacto-*N*-biose (LNB) was purchased from Elicityl SA (Crolles, France). Restriction enzymes and markers were purchased from Thermo Fisher Scientific Inc. (Waltham, MA, USA). Catalase was obtained from the Toyobo Company (175 KU/mL, Osaka, Japan). Ampicillin, kanamycin, and isopropyl- β -D-thiogalactopyranoside (IPTG) were purchased from Solarbio (Beijing, China). KOD-Plus-neo DNA polymerase (Toyobo Co., Ltd., Osaka, Japan) was used for all polymerase chain reaction amplifications. The oligonucleotides were synthesized by TsingKe (Beijing, China). All strains and plasmids in the study are listed in Table 1.

Overexpression and purification of recombinant enzymes

The genes *galk*, *ack*, *lnbp*, and *pyod* were amplified from genomic DNA of *Escherichia coli* (Yang et al., 2003; Yao et al., 2019), *Bifidobacterium bifidum* (Wada et al., 2008), and *Aerococcus viridans* ATCC 10400 (Zhang et al., 2019), respectively, then ligated with the expression vector pET28a via Red-ET recombineering method in *E. coli* strain GB05-dir (Fu et al., 2012). The constructed plasmids (pET-*galk*, pET-*lnbp*, pET-*ack*, and pET-*pyod*) were transformed into *E. coli* BL21(DE3) to generate the respective bacterial strains.

For overproduction of proteins, cells harboring the desired plasmid were grown in LB medium supplemented with 50 μ g/mL kanamycin. Cultures were grown to an OD₆₀₀ of 0.4-0.8 at 37°C and then 0.1-1 mM isopropyl β -D-thiogalactopyranoside (IPTG) was added to promote protein expression. All enzymes were purified via a Ni-NTA affinity column according to the manufacturer's instruction (Qiagen, Valencia, CA), and the resultant proteins were dialyzed against 50 mM Tris-HCl (pH 7.0) with 10% glycerol.

Enzyme activity assays

The activity of Galk (EC 2.7.1.6) was measured at 37°C for 15 min in a reaction solution including 100 mM Tris-HCl (pH 7.0), 8 mM galactose, and 10 mM ATP (Yang et al., 2003), and the reaction was stopped by boiling for 10 min. The concentration of galactose was assayed by DNS methods. One unit of enzyme activity was defined as the amount of enzyme that consumed 1 μ mole of galactose per min.

The activity of LnbP (EC 2.4.1.211) was assayed at 37°C for 10 min in a reaction solution containing 100 mM Tris-HCl (pH 7.0), 10 mM Gal-1p, and 12 mM GlcNAc (Derensy-Dron et al., 1999), and the reaction was stopped by boiling for 10 min. The product inorganic phosphate released from Gal-1p was determined using the mild pH phosphate assay as previously described (Saheki et al., 1985). One unit of enzyme activity was defined as the amount of enzyme that generated 1 nmole of inorganic phosphate per min.

The activity of AcK (EC 2.7.2.1) was determined at 37°C for 5 min in a reaction solution including 100 mM Tris-HCl (pH 7.0), 10 mM acetyl phosphate, and 5 mM ADP (Yoshioka et al., 2014), and the reaction was stopped by boiling for 10 min. The generated ATP was measured using an Enhanced ATP Assay Kit (Beyotime Biotechnology, Shanghai, China) based on the luciferin-luciferase fluorescence reaction using recombinant luciferase. Luminescence was measured using an ATP Lumitester C-110 luminometer supplied by the Kikkoman Corporation (Kikkoman Biochemifa Company, Minato-ku, Japan) (Wang et al., 2013). After the reaction was completed, 20 μ L of reaction mixture appropriately diluted with ATP detection reagent diluent was added to the 100 μ L detection reagent. Luminescence of the mixture was then measured using a Lumitester C-110 and the relative luminescent unit (RLU) value was measured as ARLU. Control reactions were conducted without AcK and the resultant

RLU was defined as B_{RLU} . AcK activity was calculated as ΔRLU ($A_{RLU}-B_{RLU}$) using ATP as the standard. One unit of enzyme activity was defined as the amount of enzyme that generated 1 nmole of ATP per min.

The activity of PyoD (EC 1.2.3.3) was determined at 37°C for 10 min as previously reported (Dai et al., 2018). After preparing the reagent A-N, the reaction components were mixed and then monitored at A_{565} nm step by step based on the reported methods (Toyo Jozo Co., 1982). One unit of enzyme activity was defined as the amount of enzyme that produced 1 μ mole of H_2O_2 per min during the conversion of pyruvate and phosphate to acetyl phosphate and CO_2 .

The kinetic parameters K_m for GalK was determined at 37°C with 100 mM Tris-HCl (pH 7.0), 10 mM ATP, various concentrations of galactose (0.5 to 20 mM), and 0.1 mg of purified GalK for 20 min. The kinetic parameters K_m for LnbP was determined at 37°C with 100 mM Tris-HCl (pH 7.0), 5 mM GlcNAc, various concentrations of Gal-1p (0.5 to 15 mM), and 0.1 mg of purified LnbP for 20 min. The kinetic parameters K_m for AcK was determined at 37°C with 100 mM Tris-HCl (pH 7.0), 5 mM ADP, various concentrations of acetyl phosphate (1 to 20 mM), and 0.12 mg of purified AcK for 20 min. The kinetic parameters K_m for PyoD was determined at 37°C with 100 mM Tris-HCl (pH 7.0), 10 mM pyruvate, various concentrations of inorganic phosphate (1 to 30 mM), and 0.2 mg of purified PyoD for 20 min. The reactions were stopped by boiling for 10 min and analyzed using the methods mentioned above.

Analytical methods

The growth of *E. coli* BL21(DE3) was determined through the optical density (OD_{600}) with a spectrophotometer (U-T1810, Yipu Instrument Co., Ltd Shanghai, China) as reported elsewhere (Guo et al., 2018). Protein concentrations were determined by the

Bradford method using bovine serum albumin as the standard.

The concentrations of galactose, GlcNAc and LNB were determined by HPLC equipped with a refractive index detector using an Aminex HPX-87H column (300 × 7.8 mm, Bio-Rad Laboratories, Hercules, CA). The mobile phase was 5 mM H₂SO₄, and samples were separated at 45°C at a flow rate of 0.6 mL/min. Retention times of galactose, GlcNAc and LNB were 11.53, 13.71, and 10.88 min, respectively (Figure S2A, Supporting Information). HPLC-MS was performed on a Thermo Scientific Dionex UltiMate 3000 LC system and a Maxis Impact HD Mass Spectrometer with an ESI ionization probe. The positive mode was used to detect LNB in the mass range of 100-800 m/z, and the data from MS (M+H)⁺: 384.29; (M+Na)⁺: 406.34; calculated MS: 383.15; molecular formula: C₁₄H₂₅NO₁₁ (Figure S2B, Supporting Information).

Optimization of cascade reaction conditions

The proof-of-concept biosynthesis pathway I & II-conditions (1 mL) was listed in Table S1 and conducted at 30°C for 12 h, respectively. Then, the reaction was stopped by boiling for 10 min. After centrifugation, the concentration of LNB in the supernatant was measured by HPLC.

Next, the effects of temperature (25, 30, 37, and 40°C), pH (6.0, 6.5, 7.0, and 8.0), Mg²⁺ (5, 10, 20, 40, and 50 mM), Tris-HCl (50, 100, 150, 200, 250, and 400 mM) and ATP (2.5, 5, 7.5, and 10 mM) at 30°C for 12 h on LNB production were investigated to obtain the optimal reaction conditions based on pathway II-condition I. First, the enzymes GalK, LnbP, AcK, PyoD and CAT were increased to 2.5 or 5 U/mL, respectively; In addition, the enzymes GalK, LnbP, AcK, PyoD and CAT were decreased to 0.1 U/mL, respectively. The influence of the loading amounts on LNB synthesis was measured. Loading amounts of PyoD (2, 10, and 20 U/mL) were employed to investigate the influence of LNB and Pi concentrations in the reaction

mixture based on the pathway II-condition II. A 100-mL reaction mixture containing 15 mM Gal, 5 mM ATP, 10 mM pyruvate, 7.5 mM GlcNAc, 100 mM Tris-HCl (pH 7.0), 10 mM MgCl₂, 2 U/mL (Galk, LnbP, AcK, and CAT), and 10 U/mL PyoD was incubated at 30°C for 48 h. The reaction mixture was stopped by boiling for 10 min, and the concentration of LNB in the supernatant was measured by HPLC after centrifugation. The LNB conversion ratio based on the GlcNAc was calculated using the $\frac{\text{mol}_{\text{[LNB]}}}{\text{mol}_{\text{GlcNAc}}}$ formula. The specific LNB yield based on the GlcNAc was calculated using the $\frac{\text{g}_{\text{[LNB]}}}{\text{g}_{\text{[GlcNAc]}} \cdot \text{h}}$ formula. Data were obtained at least in triplicate and expressed as mean \pm standard deviation.

Supplemental reference

Dai, Z. J.; Huang, M. T.; Chen, Y.; Siewers, V.; and Nielsen, J. (2018). Global rewiring of cellular metabolism renders *Saccharomyces cerevisiae* Crabtree negative. *Nat. Commun.* *9* (1), 3059-3066.

Derensy-Dron, D.; Krzewinski, F.; Brassart, C.; and Bouquelet, S. (1999). β -1,3-Galactosyl-*N*-acetylhexosamine phosphorylase from *Bifidobacterium bifidum* DSM 20082: characterization, partial purification and relation to mucin degradation. *Biotechnol. Appl. Bioc.* *29* (1), 3-10.

Fu, J.; Bian, X. Y.; Hu, S. B.; Wang, H. L.; Huang, F.; Seibert, P. M.; Plaza, A.; Xia, L.; Müller, R.; Stewart, A. F. et al. (2012). Full-length RecE enhances linear-linear homologous recombination and facilitates direct cloning for bioprospecting. *Nat. Biotechnol.* *30* (5), 440-446.

Guo, W.; Huang, Q. L.; Feng, Y. H.; Tan, T. C.; Niu, S. H.; Hou, S. L.; Chen, Z. G.; Du, Z. Q.; Shen, Y.; and Fang, X. (2020). Rewiring central carbon metabolism for tyrosol and salidroside production in *Saccharomyces cerevisiae*. *Biotechnol. Bioeng.* *117*, 2410-2419.

Saheki, S.; Takeda, A.; and Shimazu, T. (1985). Assay of inorganic phosphate in the mild pH range, suitable for measurement of glycogen phosphorylase activity. *Anal. Biochem.* *148* (2), 277-281.

Toyo Jozo Co. (1982). Ltd. Enzymatic assay of pyruvate oxidase (EC 1.2.3.3) from *Pediococcus species*. *Enzyme Handbook*. 23-24.

Wada, J.; Ando, T.; Kiyohara, M.; Ashida, H.; Kitaoka, M.; Yamaguchi, M.; Kumagai, H.; Katayama, T.; and Yamamoto, K. (2008). *Bifidobacterium bifidum* lacto-*N*-biosidase, a critical enzyme for the degradation of human milk oligosaccharides with a type 1 structure. *Appl. Environ. Microb.* *74* (13), 3996-4004.

Wang, M. Y.; He, D. D.; Liang, Y.; Liu, K. M.; Jiang, B. J.; Wang, F. Z.; Hou, S. L.; and Fang, X.

(2013). Factors involved in the response to change of agitation rate during cellulase production from *Penicillium decumbens* JUA10-1. *J. Ind. Microbiol. Biot.* *40* (9), 1077-1082.

Yang, J.; Fu, X.; Jia, Q.; Shen, J.; Biggins, J. B.; Jiang, J. Q.; Zhao, J. J.; Schmidt, J. J.; Wang, P. G.; and Thorson, J. S. (2003). Studies on the substrate specificity of *Escherichia coli* galactokinase. *Org. Lett.* *5* (13), 2223-2226.

Yao, Y. F.; Ding, Q. B.; and Ou, L. (2019). Biosynthesis of (deoxy)guanosine-5'-triphosphate by GMP kinase and acetate kinase fixed on the surface of *E. coli*. *Enzyme Microb. Tech.* *122*, 82-89.

Yoshioka, A.; Murata, K.; and Kawai, S. (2014). Structural and mutational analysis of amino acid residues involved in ATP specificity of *Escherichia coli* acetate kinase. *J. Biosci. Bioeng.* *118* (5), 502-507.

Zhang, J. G.; Lu, J. W.; and Su, E. Z. (2019). Soluble recombinant pyruvate oxidase production in *Escherichia coli* can be enhanced and inclusion bodies minimized by avoiding pH stress. *J. Chem. Technol. Biot.* *94* (8), 2661-2670.